Self-consistent simulations of a four-gated vertical quantum dot

Philippe Matagne and Jean-Pierre Leburton
Beckman Institute for Advanced Science & Technology and Department of Electrical and Computer Engineering, University of Illinois at Urbana-Champaign, Urbana, Illinois 61801
(Received 28 August 2001; published 27 March 2002)

We present three-dimensional (3D) finite-element simulations of symmetric and asymmetric chargings of a four-gated vertical quantum dot (4GVQD) structure. Emphasis is placed on 3D device effects with no *a priori* assumption about, the shape of the electron confining potential (CP). We show that, by acting asymmetrically on the electric gates, small elliptic deformations in the electron CP are induced with little changes in the addition energy spectrum of the 4GVQD. Charging spin sequences are, however, strongly modified by small deformations, and can therefore be controlled electrostatically by tuning the gates accordingly.

DOI: 10.1103/PhysRevB.65.155311 PACS number(s): 73.21.-b, 72.20.My, 73.40.Gk

I. INTRODUCTION

The electronic properties of quantum dots (QD's) recently became a topic of major interest, since QD's show basic properties of a few electron systems, and are promising candidates for future device applications.[1] A significant experimental and theoretical effort has been devoted to the study of highly symmetric cylindrical structures, which demonstrated the existence of atomiclike properties of the confined electrons such as orbital motion, three-dimensional (3D) energy quantization, shell structure, and the Hund's rule.[2–9] However, these ideal features are very sensitive to the electrostatic potential confining the electrons.[10–12] In particular, a disruption of the potential symmetry can alter the electronic configuration of the dot. Recently, Austing and co-workers investigated a square vertical quantum dot (VQD) with four independent gates,[13,14] that causes a deformation of the lateral potential by acting differently on each gate. The interest in this study was to analyze the influence of the spatial distortion of the lateral confinement on the atomiclike properties of the VQD. Evidence of the deformation of the confining potential (CP) was deduced from measurements of the source-drain current peak spacing, which arises from single-electron tunneling between Coulomb blockade regimes, as a function of the gate voltages. In particular, it was found that the peak spacings were more separated when fewer gates were operated, evidencing different CP's for different gate voltage sequences. Later on, Austing *et al.* experimentally and theoretically studied the charging of rectangular QD's with aspect ratios (δ) varying from 1 to 3.2.[11] A similar theoretical study was also performed by Lee, Kim, and Ahn,[10] for $1 \leqslant \delta \leqslant 2$. Both works assume an *a priori*, lateral CP given by $V_{ext} = \frac{1}{2}\omega^2[\delta x^2 + (y^2/\delta)]$, and show that, for an ellipticity factor $\delta > 1.2$, the shell structure is almost completely destroyed and the total spin sequence is strongly altered.

In this paper, we perform a 3D analysis of a four-gated QD where the CP is not assumed *a prior* but directly deduced from the boundary conditions in the nanostructure varying with applied gate biases. For this purpose, we carry out a 3D self-consistent computer simulation of the VQD by taking into account the full device structure, the effect of the equipotential, and many-body interactions. We use finite element solutions of the coupled Poisson- and Schrödinger-like (Kohn-Sham) 3D equations within the density-functional theory suitable to simulate an arbitrary number of electrons in the VQD. This approach allows us to predict the strength of the deformation in the dot by manipulating the CP electrostatically. Specifically, we show that the deformations induced electrostatically are much weaker ($\delta \approx 1.1$) than those obtained in rectangular QD's with large aspect ratios.[10,11] Hence four-gated structures provide a very fine electrostatic control of the deformation on the orbitals and, in particular, on the total spin of the system. However, unlike previous findings on large QD ellipticity,[7,11] we show that the addition energy spectrum $E_a(N)$, i.e., the chemical potential difference between $N+1$ and N electrons $[E_a = \mu(N+1) - \mu(N)]$, as a function of the number of electrons N in the dot, is not very sensitive to small deformations.

II. FOUR-GATED SQUARE VERTICAL QUANTUM DOT (4GVQD) STRUCTURE

Figure 1(a) shows a schematic view of a 4GVQD with an 0.8μ side length similar to the device investigated by Austing, Honda, and Tarucha.[13] It consists of an undoped 12-nm $In_{0.05}Ga_{0.95}As$ well and undoped $Al_{0.22}Ga_{0.78}As$ barriers of thicknesses 9 and 7.5 nm. The lead on the side of the thinner (thicker) tunnel barrier is made of n^+-type GaAs, and is referred to as the source (drain). In this paper, we focus exclusively on a regime close to equilibrium, so that the electronic structure of the QD is unaffected by the drain-source bias. The doping is gradually reduced from $N_D = 2\,10^{18}/\mathrm{cm}^3$ at the source (drain) to $N_D = 10^{17}/\mathrm{cm}^3$ at the double-barrier heterostructure over a distance of 4000 Å. The top view [Fig. 1(b)] reveals the four independent Schottky gates *A*, *B*, *C*, and *D* with corresponding voltages V_A, V_B, V_C, and V_D. Sweeping the gates continuously leads to an alternation of Coulomb blockade and single-electron tunneling events.[15] In the former regime, the number of electrons in the dot N is fixed, while in the latter the number of electrons fluctuates between N and $N+1$. By calculating the equilibrium configurations of the QD, we determine the most favorable number of electrons in the dot for a

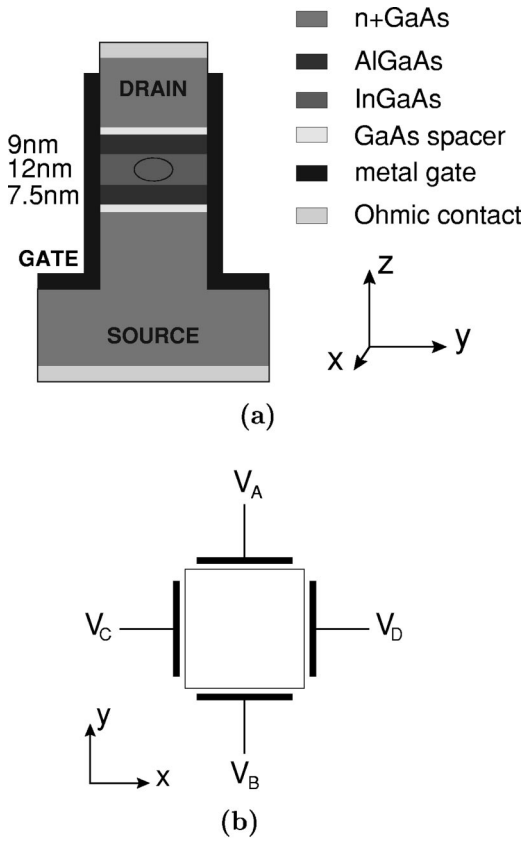

FIG. 1. (a) Schematic diagram of a vertical quantum dot tunneling heterostructure showing the different semiconductor layers. The quantum dot, represented by the oval, lies in a 12-nm wide quantum well ($In_{0.05}Ga_{0.95}As$) surrounded by two potential barrier ($Al_{0.22}Ga_{0.78}As$) whose thicknesses are 7.5 nm on the source side and 9 nm on the drain side. (b) Top view showing the four independent gates with applied voltages V_A, V_B, V_C, and V_D.

given bias. Therefore, we can obtain the various biases at which a transition $N \rightarrow N+1$ occurs.

III. NUMERICAL MODEL

The electron density in the QD is obtained by solving two Kohn-Sham equations in order to take into account the spin dependence on the electron-electron interaction. The Hamiltonians read

$$H^{\uparrow(\downarrow)}(\mathbf{r}) = -\frac{\hbar^2}{2}\nabla\left[\frac{1}{m^*(\mathbf{r})}\nabla\right] - q\phi(\mathbf{r}) + \Delta E_c + \phi_{xc}^{\uparrow(\downarrow)}(n) \tag{1}$$

where $m^*(\mathbf{r})$ is the position-dependent effective mass. $\phi(\mathbf{r}) = \phi_{ext} + \phi_{ion} + \phi_H$ is the electrostatic potential which consists of three contributions: ϕ_{ext} is the potential due to an external applied bias, ϕ_{ion} is the potential resulting from ionized donors in the vertical structure, and ϕ_H is the Hartree potential accounting for repulsive electron-electron interactions. ΔE_c is the conduction-band offset between different materials, i.e., 181 meV for $Al_{0.22}Ga_{0.78}As/GaAs$ and 35 meV for $GaAs/In_{0.05}Ga_{0.95}As$, and $\phi_{xc}^{\uparrow(\downarrow)}$ is the exchange and correlation potential energy for spin up ($\uparrow$) and down ($\downarrow$) that is computed within the local-spin-density approximation (LSDA) according to Perdew and Wang's formulation.[16] The LSDA approach to the study of the electronic structure of quantum dots has been well tested by many authors.[17–20] It successfully explains the quasi two-dimensional shell structures and spin configurations of QD's, and is in good agreement with 2D quantum Monte Carlo simulations.[21,22] Moreover, applications of the LSDA to few-electron atoms has shown an accuracy on the order of 1% in the calculations of the atom's ionization energy.[23] The electrostatic potential $\phi(\mathbf{r})$ is computed by solving Poisson's equation. In the leads, $n(\mathbf{r})$ is assumed to be semi-classical and described by the Thomas-Fermi model. Kohn-Sham and Poisson equations are discretized by the finite-element method, and solved with appropriate boundary conditions for which a detailed formulation was published elsewhere.[6]

Finally, in order to determine N, we use the Slater formula[24]

$$E_T(N+1,V_G) - E_T(N,V_G) = \int_0^1 \varepsilon_{LUO}(n)dn \approx \varepsilon_{LUO}(1/2) - E_F, \quad N = 0,1,\ldots \tag{2}$$

where $E_T(N)$ is the total energy for N electrons in the dot, ϵ_{LUO} is the lowest unoccupied orbital eigenvalue, E_F is the Fermi energy, and V_G is the gate voltage for a particular bias between the A, B, C, and D electrodes. Hence the most favorable configuration, i.e., the lowest in energy, consists of the configuration with N electrons inside the dot if the integral of Eq. (2) is positive, $N+1$ electrons otherwise. The procedure consists in starting with an empty dot and charging it successively with electrons by increasing the gate voltage(s). At each V_G step, Eq. (2) checks the most favorable number of electrons in the dot.

IV. RESULTS

Figure 2 shows the source-drain current peak spacing as a function of the gate voltage V_G and the number of electrons, N, inside the dot for two different gate voltage sequences. Each peak, schematically represented by a vertical arrow, corresponds to an additional electron in the dot. The arrow orientation indicates the spin polarity. The peak height is arbitrary, since our model does not compute the transport properties. For each sequence, the total spin S as a function of N in the dot is shown on the inset. In Fig. 2(a), the VQD is pinched off with the four gates at $V_G = -2.98$ V. Then the four gates are interconnected and swept continuously from -2.98 V to -2.73 V to charge 13 electrons in the dot (symmetric charging). If ΔV_G^i denotes the incremental gate voltage required to add the ith electron in the dot, the large gaps ΔV_G^3, ΔV_G^7, and ΔV_G^{13} reflect the shell structure of the orbitals proper to the quasiparabolic confining potential of a symmetrical structure.[2,7,6] For $N=4$ and 9 and $S=1$ and 3/2, respectively, e.g., the dot is fully polarized at half occupied shells because these configurations are more favorable with

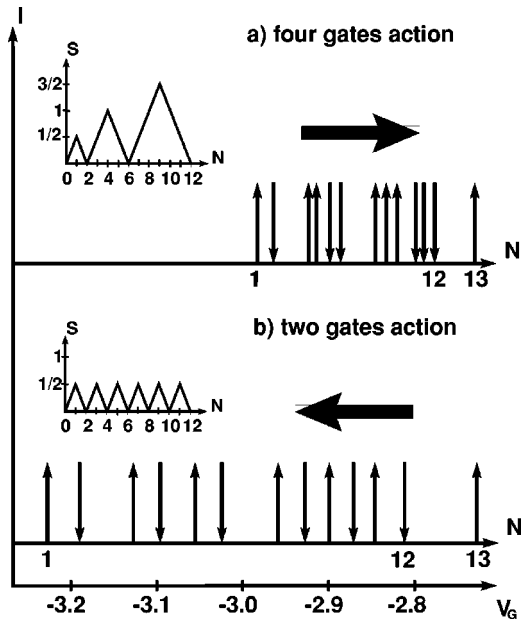

FIG. 2. Source-drain current peak spacing as a function of the gate voltage V_G and the number of electrons N (a) when the four gates are swept uniformly, and (b) when only V_C and V_D are swept while V_A and V_B are held at $V_G=-2.73$ V. Inset: total spin S of the QD as a function of N.

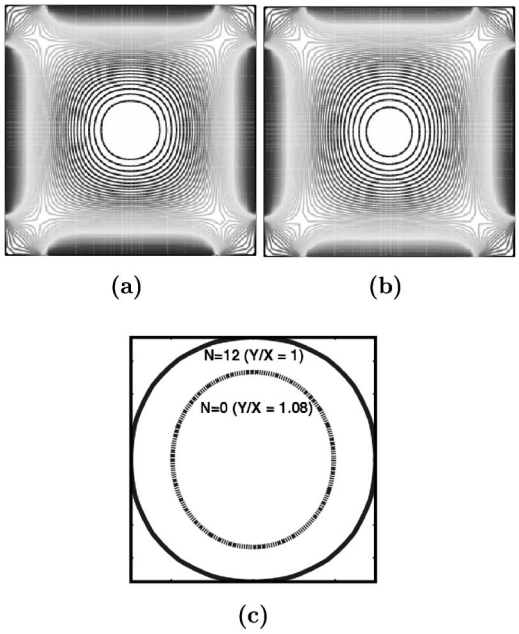

FIG. 3. X-Y potential contour plots (a) for $N=12$ and $V_A=V_B=V_C=V_D=-2.8$ V, and (b) for $N=0$, $V_A=V_B=-2.73$ V and $V_C=V_D=-3.24$ V. (c) potential contour at $\phi=E_F/q$ for $N=12$ (solid line) and $N=0$ (dashed line).

electrons of parallel spins (exchange energy is maximized) and orthogonal orbitals (Hartree energy is minimized).[12] In Fig. 2(b), the two opposite gates A and B are kept at a constant voltage $V_A=V_B=-2.73$ V, and V_C and V_D are swept backward until the dot is again empty at $V_G=-3.24$ V (asymmetric charging). We first note that the gate voltage swing with two acting gates is almost exactly twice the gate voltage swing for four acting gates, reflecting the fact that the strength of four gates is twice that of two gates, which confirms the experiments. This effect can also be noted by observing that the separation between individual peaks is larger when only two gates are swept. In this respect, it is interesting to compare ΔV_G^j and ΔV_G^k, where the $(j-1)$th and jth electrons belong to the same shell, whereas the $(k-1)$th and kth electrons belong to different shells. In both Figs. 2(a) and 2(b), $\Delta V_G^k > \Delta V_G^j$, i.e., the shell structure is preserved even in the asymmetric charging. However, the ratio $\Delta V_G^k/\Delta V_G^j$ is smaller in the asymmetric configuration, which indicates that the shell structure is weaker when the CP loses symmetry. As seen in the inset of Fig. 2(b), the total spin of the dot reveals orbitals filling successively with electrons of antiparallel spins. Indeed, due to the CP deformation, the degeneracies inside a shell are gradually lifted and, at some point, sequential state filling with antiparallel spin electrons becomes more favorable because an exchange between electrons no longer compensates for the degeneracy lifting between occupied levels.

Figure 3 shows the equipotential contours in the X-Y plane of the dot, for $N=12$ at $V_G=-2.73$ V [Fig. 3(a)], when the dot is still uniformly biased, and for $N=0$ and $V_C=V_D=-3.25$ V [Fig. 3(b)], after the asymmetric bias has been applied. In both cases, the very dense equipotentials on the four sides of the plots denote the proximity of the gates. In Fig. 3(a), the contours are circular at the center, and become square at the periphery, while in Fig. 3(b), they become slightly elliptic in the center, which reflects the fact that the electric field is now stronger in the x direction than in the y direction. However, the deformation is weak, as shown in Fig. 3(c), where the equipotential is drawn at the Fermi level before (solid line, $N=12$) and after deformation (dashed line, $N=0$). The area spanned by the Fermi contours reflects the effective size of the QD. Since the solid (dashed) contour corresponds to $N=12$ ($N=0$), it simply shows that the QD expands while filled with electrons. It is also worth noting that, at $T=0$ K, the electronic properties are mainly determined by the confining potential at the Fermi level, which explains why large square and circular QD's have almost identical electronic properties, as already reported by Kumar *et al.*[25] The aspect ratio of the dot after deformation is $\delta=1.08$, for a gate voltage swing ratio of $\Delta V_G=0.49/0.25=1.96$, which shows that we cannot expect to obtain large deformations in electrostatic deformable dots as opposed to rectangular dots, where δ, determined by the geometric aspect ratio, is arbitrarily fixed.

Figure 4 shows the contour plots of the first six eigenfunctions as a function of the number of electrons in the case of asymmetric voltage sweep. The uppermost row corresponds to $N=12$, before deformation ($V_A=V_B=V_C=V_D=-2.73$ V), and the lowermost row corresponds to $N=0$ ($V_A=V_B=-2.73$ V and $V_C=V_D=-3.24$ V), i.e., the strongest deformation. Intermediate rows show the progressive transformation from circularly confined orbitals to elliptically confined orbitals as N varies from 12 to 0. Before deformation, the first orbital is an s-like state according to atomic physics, and constitutes the first shell. The second

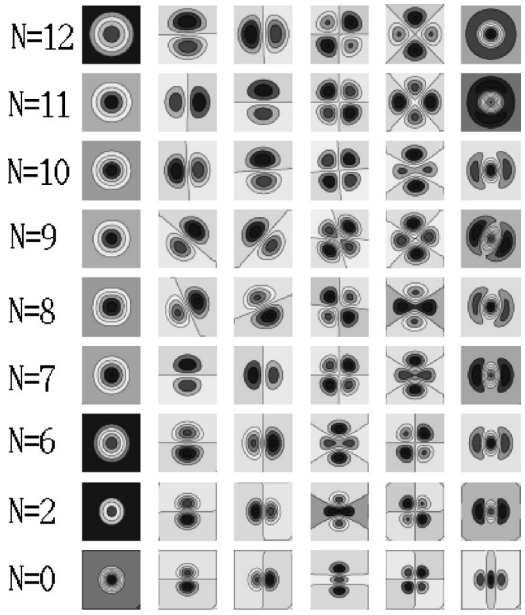

FIG. 4. Wave-function contour plots for the first three shells (first shell: first column; second shell: second and third column; third shell: fourth, fifth, and sixth columns) of a 4GVQD. From the top row to the bottom row, N varies from 12 to 0, V_C and V_D are swept from -2.8 to -3.24 V. V_A and V_B are help at -2.73 V.

and third orbitals are p like, and form the second shell. The fourth and fifth d-like orbitals, and the sixth s-like orbital, form the third shell. In general, all the orbitals are less spread out for $N=0$ than for $N=12$ because, as mentioned above, the dot has shrunk.

The first orbital is very weakly affected by the deformation. From $N=12$ to 8, the two p states do not show any particular favored orientation. Physically, as long as they are degenerate, all linear combinations of the original eigenfunctions are equally valid solutions. Numerically, the orientation of the two degenerate wave functions is mainly influenced by the mesh. Conversely, from $N=7$ to 0, V_A and V_B are now substantially different than V_C and V_D, so that the states are no longer degenerate and align according to the symmetry axis of the dot. The third-shell orbitals (last three columns) show the most spectacular transformations, i.e., from circular state symmetry with principal and azimuthal quantum numbers $(n,l)=(0,2)$, $(0,-2)$, and $(1,0)$ to rectangular state symmetry with quantum numbers $(n_x,n_y)=(0,2)$, $(1,1)$, and $(2,0)$ states, respectively. One also notes the crossing between the fourth and fifth eigenlevels at the transition $N=7\rightarrow 6$.

Various addition energy spectra (AES's), i.e., the chemical potential difference between $N+1$ and N electrons $[E_a=\mu(N+1)-\mu(N)]$, as a function of the number of electrons N, are shown in Fig. 5. Figure 5(a) shows a comparison between the theoretical AES corresponding to the symmetric charging (dashed line) and the AES corresponding to the asymmetric charging (solid line). The symmetric and asymmetric AES's have similar global features. First there are large peaks at $N=2$, 6, and 12 due to the shell structure, which reflects the energy contribution needed to lower the

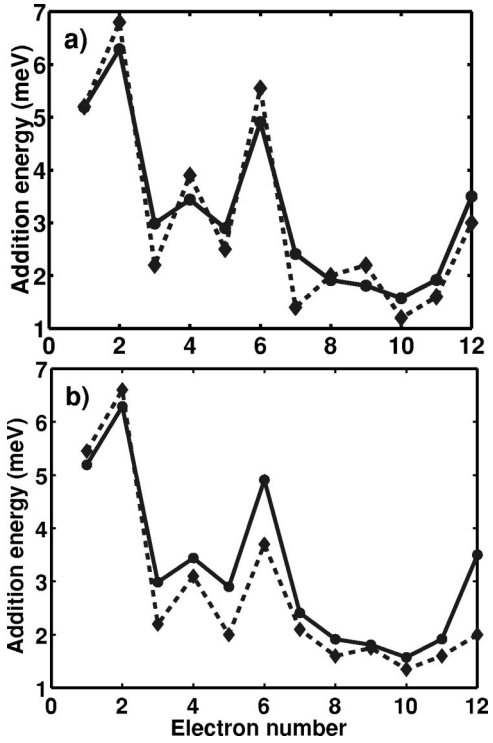

FIG. 5. (a) Theoretical addition energy spectra of 4GVQD for symmetric charging (dashed) and asymmetric charging (solid) as functions of the number of electrons. (b) Comparison between computed addition energy spectrum (solid) of the asymmetric 4GVQD and the experimental spectrum (Ref. 2) of a symmetric VQD (dashed) as a function of the number of electrons. Note that, by definition, $E_a(N)=E_F(N+1)-E_F(N)$, so that a value for $N=j$ in this figure refers to the energy needed to add the $(j+1)$th electron in the dot.

next orbital below the Fermi level for admitting the next electron, in addition to the energy required to overcome the electrostatic repulsion of the electrons already present in the dot. These peaks are approximately 0.5 meV lower in the asymmetric AES, however, since the intershell spacing is reduced in this configuration. Second, there are secondary peaks at $N=4$, which was explained so far in terms of Hund's rule (HR) (Refs. 2 and 7): the third and fourth electrons, with parallel spins ($\uparrow$), access empty p-like orbitals, maximize E_{xc}, and minimize E_H, inducing a minimum for $N=3$. For $N=4$, the fifth electron with antiparallel spin sits on an already occupied state, which increases E_H. Moreover, this electron is the only $\downarrow$ electron in the second shell, with no additional exchange interaction; thus $E_a(4)>E_a(3)$. For $N=5$, the sixth electron sits on an already occupied orbital, sharing an exchange interaction with the fifth electron, which lowers $E_a(5)<E(4)$, leading to a peak for $N=4$. This explanation applies, of course, to the symmetric AES [solid curve, Fig. 5(a)], which demonstrates that HR is a necessary condition for observing a peak at $N=4$. However, it is not a sufficient condition, since the asymmetric AES [dashed curve, Fig. 5(a)] also exhibits a peak at $N=4$, and, as shown before, HR is not fulfilled for asymmetric charging [inset of Fig. 2(b)]. The peak is weaker, however, since there is no exchange between the third (fifth) and fourth (sixth) peaks,

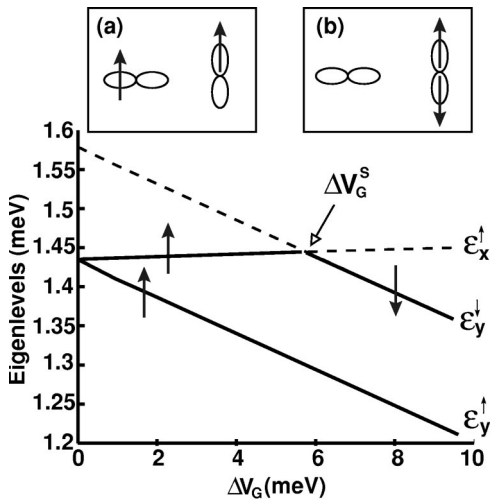

FIG. 6. Variation of the single-particle eigenlevels of the second shell $\epsilon_x^{\uparrow}$, $\epsilon_y^{\uparrow}$, and $\epsilon_y^{\downarrow}$ as a function of $\Delta V_G \equiv V_X - V_Y$ ($X=A,B$; $Y=C,D$). A solid (dashed) eigenlevel is connected to an occupied (empty) orbital. For $\Delta V_G < \Delta V_G^S = 5.8$ meV, two parallel electron spins) sit on the orbitals associated with $\epsilon_x^{\uparrow}$ and $\epsilon_y^{\uparrow}$, so that the favored configuration is shown in the top left inset, i.e., a triplet state. For $\Delta V_G > \Delta V_G^S$, two antiparallel electron spins sit on the orbitals associated with $\epsilon_y^{\uparrow}$ and $\epsilon_y^{\downarrow}$, so that the favored configuration is shown on the top right inset, i.e, a singlet state ($S=0$).

which increases the addition energy for $N=3$ and 5. Moreover, the fifth electron now sits on an unoccupied orbital, which reduces the addition energy for $N=4$. For the symmetric charging, there is also a secondary peak for $N=9$ which, with a dip at $N=7$, reflects three parallel spins in the third shell.[26,27] This peak is not present in the asymmetric AES, which shows that, due to symmetry breaking, levels are more randomly distributed inside the third shell. In summary, a secondary peak in the energy spectrum is not necessarily the signature of parallel spin alignment.

Figure 5(b) shows a comparison between the theoretical asymmetric charging (solid) and experimental AES's of a circular device.[2] The striking feature here is that the asymmetric AES very closely follows the experimental AES of the cylindrical structure. The asymmetric AES is actually closer to the experimental AES than the symmetric AES, in particular for third-shell charging. This agreement is not fortuitous, since it was recently demonstrated that the peak structure in the experimental curve[2] reflects a sequence of alternate spins in the filling of the third shell,[26] similar to the sequence achieved in the theoretical asymmetric charging. This observation leads us to conclude that real VQD's are probably never completely symmetric.

Based on the observations above, and on the fact that the total energy of the dot is spin dependent, we investigate the possibility of changing the spin polarization by deforming the dot electrostatically (Fig. 6).[28] Here we assume that the first shell is completely filled, and we exclusively focus on filling the second shell, which consists of two degenerate *p*-like states, each of them being twofold spin degenerate. Let us call these $\psi_x^{\uparrow}$, $\psi_x^{\downarrow}$, $\psi_y^{\uparrow}$, and $\psi_y^{\downarrow}$ with eigenvalues $\varepsilon_x^{\uparrow}$, $\varepsilon_x^{\downarrow}$, $\varepsilon_y^{\uparrow}$, and $\varepsilon_y^{\downarrow}$, respectively. Let us assume that, with $N=3$, $\varepsilon_x^{\uparrow}$ is occupied. Now let us increase the four gates positively until the fourth electron enters the dot. By using the same argument as above, as long as the orbitals are degenerate, the energetically most favorable configuration for $N=4$ is achieved with the occupation of $\varepsilon_y^{\uparrow}$ with the fourth electron, as predicted by HR. As soon as the fourth electron is in the dot, $V_C = V_D \equiv V_Y$ is made more negative and $V_A = V_B \equiv V_X$ more positive to confine electrons more strongly along the *x*-direction than the *y* direction, while keeping $N=4$ constant. Figure 6 shows the evolution of $\varepsilon_x^{\uparrow}$, $\varepsilon_y^{\uparrow}$, and $\varepsilon_y^{\downarrow}$ with respect to $\Delta V_G \equiv V_X - V_Y$. When $\Delta V_G = 0$, the dot is spatially symmetric; hence $\varepsilon_x^{\uparrow} = \varepsilon_y^{\uparrow}$ and $\varepsilon_x^{\downarrow} = \varepsilon_y^{\downarrow}$. The dot is spin polarized, however, and the exchange energy between $\uparrow$ electrons lowers $\varepsilon_x^{\uparrow}$ and $\varepsilon_y^{\uparrow}$ with respect to $\varepsilon_x^{\downarrow}$ and $\varepsilon_y^{\downarrow}$. Another interpretation of the gap between $\varepsilon_x^{\uparrow}, \varepsilon_y^{\uparrow}$ and $\varepsilon_x^{\downarrow}, \varepsilon_y^{\downarrow}$ is given by the Coulomb blockade, that should be overcome to populate the empty orbitals. Let us mention that $\varepsilon_x^{\downarrow}$, which is equal to $\varepsilon_y^{\downarrow}$ for $\Delta V_G = 0$ and runs parallel to $\varepsilon_x^{\uparrow}$, is not shown for clarity, since it is never occupied. As $V_X(V_Y)$ is made more positive (negative), the confining potential along $y(x)$ is weaker (stronger), ε_y (ε_x) are shifted down (up), and the energy separation $\varepsilon_x^{\uparrow} - \varepsilon_y^{\uparrow}$ grows linearly. It must be noted that the rate of decrease of ε_y is larger than the rate of increase of ε_x because ΔV_Y should be smaller than ΔV_X in order to maintain four electrons inside the dot. Otherwise, if $\Delta V_Y = \Delta V_X$, the three-electron configuration is more favorable. For $V_G < V_G^S$, $\varepsilon_x^{\uparrow}$ is smaller than $\varepsilon_y^{\downarrow}$, and the parallel spin configuration, schematically shown in Fig. 6(a), is favored with respect to the configuration shown in Fig. 6(b), because the attractive exchange interaction between electrons sitting on $\psi_x^{\uparrow}$ and $\psi_y^{\uparrow}$ is larger than the energy separation $\varepsilon_x^{\uparrow} - \varepsilon_y^{\uparrow}$. At $V_G = V_G^S$, $\varepsilon_x^{\uparrow} - \varepsilon_y^{\uparrow} = 0.15$ meV exactly offsets the exchange energy between the two parallel spin electrons with wave functions $\psi_x^{\uparrow}$ and $\psi_y^{\uparrow}$. For $V_G > V_G^S$, $\varepsilon_x^{\uparrow}$ is larger than $\varepsilon_y^{\downarrow}$, i.e., the exchange interaction between parallel spin electrons is no longer capable of overcoming the energy separation $\varepsilon_x^{\uparrow} - \varepsilon_y^{\uparrow}$, and the $\psi_y^{\downarrow}$ state becomes energetically more favorable than the $\psi_x^{\uparrow}$ state. Thus, through electrostatic deformation, it is possible to control the spin polarization of a 4VGQD. This effect could be exploited for spin injection or detection in quantum information processing in a scheme involving VQD's in spin-qubit circuits.[29,30]

V. CONCLUSION

We have performed a self-consistent 3D simulation on 4GVQD's, and have shown that, by acting asymmetrically on the electric gates, it is possible to alter the electron CP, although the deformation is relatively small ($\delta = 1.08$). However, while the addition energy spectrum is relatively unchanged, the spin configuration in the QD is very sensitive to small CP deformations. Hence spin alignment cannot be solely deduced from the addition energy spectrum. Finally, we have shown that it is possible to control the total spin configuration electrostatically, without changing the electron number *N*.

ACKNOWLEDGMENTS

This work was supported by NEDO and NSF Grant No. DESCARTES ECS-98-02730. One of us (P.M.) gratefully acknowledges the support of the Beckman Institute. We are also indebted to Dr. G. Austing, Professor S. Tarucha, and Professor R. Martin for fruitful discussions.

[1] K.K. Likharev, Proc. IEEE **87**, 606 (1999).
[2] S. Tarucha, D.G. Austing, T. Honda, R.J. van der Hage, and L.P. Kouwenhoven, Phys. Rev. Lett. **77**, 3613 (1996).
[3] S. Tarucha, D.G. Austing, and T. Honda, Jpn. J. Appl. Phys. **37**, 3917 (1997).
[4] L.P. Kouwenhoven, T.H. Oosterkamp, W.S. Danoesastro, M. Eto, D.G. Austing, T. Honda, and S. Tarucha, Science **278**, 1788 (1997).
[5] S. Tarucha, D.G. Austing, Y. Tokura, W. van der Wiel, and L.P. Kouwenhoven, Phys. Rev. Lett. **84**, 2485 (2000).
[6] P. Matagne, J.-P. Leburton, J. Destine, and G. Cantraine, Comput Modeling Eng. Sci. **1**, 1 (2000).
[7] I.-H. Lee, V. Rao, R.M. Martin, and J.-P. Leburton, Phys. Rev. B **57**, 9035 (1998).
[8] M. Macucci, K. Hess, and G.J. Iafrate, Phys. Rev. B **55**, 4879 (1997).
[9] C. Yannouleas and U. Landman, Phys. Rev. Lett. **82**, 5325 (1999).
[10] I.-H. Lee, Y.-H. Kim, and K.-H. Ahn, J. Phys.: Condens. Matter **13**, 1993 (2001).
[11] D.G. Austing, S. Sasaki, S. Tarucha, S. Reimann, M. Koskinen, and M. Manninen, Phys. Rev. B **60**, 11 514 (1999).
[12] P. Matagne and J.-P. Leburton (unpublished).
[13] D.G. Austing T. Honda, and S. Tarucha, Jpn. J. Appl. Phys. **36**, 4151 (1997).
[14] D.G. Austing, T. Honda, and S. Tarucha, Semicond. Sci. Technol. **12**, 631 (1997).
[15] M. A. Kastner, Phys. Today **46**(1), 24 (1993).
[16] Y. Wang and Y. Chou, Appl. Phys. Lett. **63**, 2257 (1993).
[17] D. Jovanovic and J.-P. Leburton, Phys. Rev. B **49**, 7474 (1994).
[18] L.R.C. Fonseca, J.L. Jimenez, J.-P. Leburton, and R.M. Martin, Phys. Rev. B **57**(7), 4017 (1998).
[19] M. Macucci, K. Hess, and G.J. Iafrate, Phys. Rev. B **48**, 17 354 (1993).
[20] M. Stopa, Phys. Rev. B **54**, 13 767 (1996).
[21] F. Pederiva, C.J. Umrigar, and E. Lipparini, Phys. Rev. B **62**, 8120 (2000).
[22] J. Harting, O. Mülken, and P. Borrmann, Phys. Rev. B **62**, 10 207 (2000).
[23] R. Jones and O. Gunnarsson, Rev. Mod. Phys. **61**, 689 (1989).
[24] J. Slater, Adv. Quantum Chem. **6** (1972).
[25] A. Kumar, S.E. Laux, and F. Stern, Phys. Rev. B **42**, 5166 (1990).
[26] P. Matagne, J.-P. Leburton, D. Austing, and S. Tarucha (unpublished).
[27] P. Matagne, J.-P. Leburton, D. Austing, and S. Tarucha, Physica E (to be published).
[28] H. Ohno *et al.*, Nature (London) **408**, 944 (2000).
[29] S. Bandyopadhyay, arXiv:quant-ph/0101058 (unpublished).
[30] R. Vrijen *et al.*, Phys. Rev. A **62**, 012306 (2000).